ChemComm

Accepted Manuscript

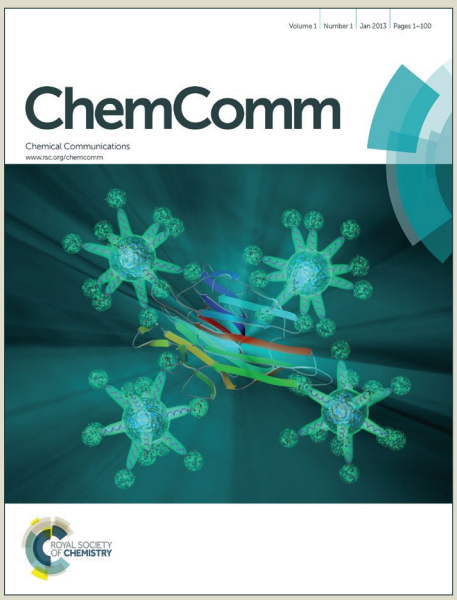

ROYAL SOCIETY OF CHEMISTRY

www.rsc.org/chemcomm

Journal Name

COMMUNICATION

Synergetic Effect Enhanced Photoelectrocatalysis

Jingchun Jia, Jie Zhang, Fangfang Wang, Lianhuan Han, Jian-Zhang Zhou, Bing-Wei Mao, Dongping Zhan*

Received 00th January 20xx,
Accepted 00th January 20xx

DOI: 10.1039/x0xx00000x

www.rsc.org/

We report synergetic effect enhanced photoelectrocatalysis, in which Fe^{3+} and Br^- are used as the acceptors of photogenerated charges on TiO_2 nanoparticles. Kinetic rate of interfacial charge transfer is promoted from $(4.0\pm0.5)\times10^{-4}$ cm/s (TiO_2/(O_2, Br^-)) to $(1.5\pm0.5)\times10^{-3}$ cm/s (TiO_2/(Fe^{3+}, Br^-)). Synergetic effect provides a valuable approach to the design of photoelectrocatalytic systems.

Sunlight is the most abundant energy resource, which is considered to be a prospective solution to the energy and environment crises caused by the world's growing population and industrialization.[1] For centuries, human beings have learnt to realize photoelectrochemical conversion using either natural or artificial materials. In 1972, Fujishima and Honda discovered photocatalytic splitting of water on illuminated TiO_2 electrodes.[2] Since then TiO_2 has been adopted intensively as photoelectrode in solar devices, and becomes the most investigated photoelectrocatalyst acting as the bridge leading solar energy to chemical energy.[3, 4]

Photoelectrochemical conversions have found many important applications including the photovoltaic devices, the pollutant decompositions as well as fuels or fine chemicals production.[5-7] Light harvest, charge separation, charge recombination, and charge transfer are the basic surface and interfacial processes in photoelectrochemical reactions, and the overall efficiency is determined by the balance of thermodynamics and kinetics of these processes.[4, 8, 9] Significant progresses have been made in the development of novel nano-photocatalysts.[10, 11] However, here we would like to emphasize the importance of interfacial reaction system on the photoelectrochemical conversion.

In fact, at photocatalyst/solution interface, redox mediators in the solution serve as charge acceptors and affect the photo-driven interfacial charge transfer. Suppose two kinds of redox mediators can accept electrons and holes respectively, the separated charges on the surface of illuminated photocatalyst will be transferred across the photocatalyst/solution interface (Figure 1a).[8] If a subsequently homogeneous chemical reaction can occur between the products of the interfacial charge transfer reactions to regenerate the redox mediators, the interfacial charge transfer will be accelerated due to the mass transfer loop (Figure 1b). We choose Fe^{3+} and Br^- as the acceptors of electrons and positive holes in experiment. When the TiO_2-nanoparticles-coated photoelectrode is illuminated by a Xenon lamp, Fe^{2+} and Br_2 are produced due to the interfacial charge transfer reactions. A subsequently homogeneous reaction between Fe^{2+} and Br_2 will occur to regenerate Fe^{3+} and Br^-. The mass transfer loop at the photocatalyst/solution interface will enhance the transfer of photogenerated charges.

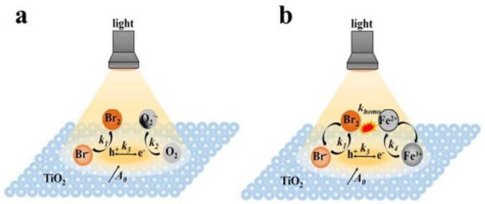

Figure 1 Schematic diagrams of (a) TiO_2/O_2/Br^- photoelectrochemical system, and (b) the synergetic effect of TiO_2/ Fe^{3+}/Br^- photoelectrochemical system.

Bromine (Br_2) is a strong oxidant used in organic synthesis, pollutant degradation and semiconductor etching, which is poisonous and dangerous for storage and transport.[12-16] The aim of this work is to provide a green method for the generation of Br_2 in situ. The first photoelectrochemical reaction system (Figure 1a) is designed by using dissolved oxygen (O_2) and Br^- as the acceptors for electrons and positive holes, respectively. Scanning electrochemical microscopy (SECM) is adopted to detect the interfacial concentration distribution of photogenerated Br_2 (See S1). When the photoelectrode is illuminated, the following reaction occurs:[17, 18]

$$O_2 + e^- \rightarrow O_2^{\bullet-} \quad (1)$$

$$Br^- + h^+ \rightarrow 1/2\,Br_2 \quad (2)$$

The apparent photoelectrochemcial conversion rate can be deduced as followed (details see S2)[19, 20]:

$$r = K_a[Br^-]^{1/2}[O_2]^{1/2} \quad (3)$$

where, K_a is the apparent kinetic rate of interfacial charge transfer, [Br^-] and [O_2] are the interfacial concentration of Br^- and O_2.

[a] State Key Laboratory for Physical Chemistry of Solid Surfaces and Department of Chemistry, College of Chemistry and Chemical Engineering, Xiamen University, Xiamen 361005, China.
E-mail, dpzhan@xmu.edu.cn; tel, +865922185797; fax, +865922181906.
† Electronic Supplementary Information (ESI) available. See
DOI: 10.1039/x0xx00000x

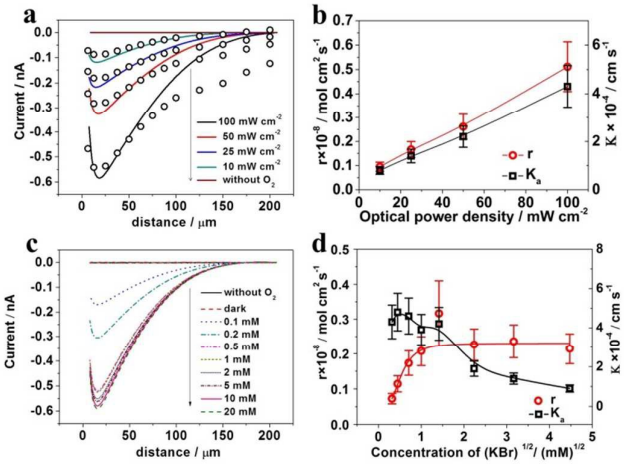

Figure 2 (a) Approach curves obtained in 0.05 M H_2SO_4 and 10 mM KBr solution with different illumination intensity (line: experimental, spot: simulated). (b) Relationship between light intensity and the simulated apparent rate *r* (o) as well as apparent rate constant K_a (□) in 0.05 M H_2SO_4 and 5 mM KBr solution. (c) Approach curves obtained in 0.05 M H_2SO_4 solutions with different concentration of KBr ranging from 0.1 mM to 20 mM KBr, light intensity is 100 mW/cm^2. (d) Relationship between the concentration of KBr and the simulated apparent rate *r* (o) as well as apparent rate constant K_a (□). All the solutions are O_2 saturated, tip potential is held at 0.7 V vs. Ag/AgCl reference electrode in experiment.

To ensure the sufficient mass transfer flux and the reproducibility of the experiments, the electrolyte is saturated with O_2 by bubbling air gently. Figure 2a shows the approach curves obtained in O_2-saturated aqueous solution with 10 mM KBr and 0.05 M H_2SO_4 at different illumination intensity. If the solution is degased with pure nitrogen gas (N_2) to eliminate the dissolved O_2, the photochemical processes will not happen due to the lack of electron acceptor. Once the TiO_2 is illuminated in the O_2-saturated solution, the increasing feedback current is observed with the decreased tip-substrate distance. However, the feedback current decreases when the tip-substrate distance is less than 20 μm. This is caused by the hindered mass transfer of O_2 from bulk solution into the thin layer between tip and substrate. Figure 2b indicates the interfacial charge transfer rate is in proportion to the illumination intensity. The details of kinetic simulations can be seen in S2.

Due to the limited solubility in aqueous solution, the interfacial charge transfer rate might be determined by either mass transfer or charge transfer of O_2. That means the catalytic capability of TiO_2 photocatalyst is not utilized sufficiently. To clarify this point, experiments are performed with a series of [Br^-] as shown in Figure 2c. Simulation results show that the apparent photoelectrochemical conversion rate of Br^- oxidation (r) becomes constant when [Br^-] is higher than 1.0 mM. In the kinetic region (i.e., 0 < [Br^-] < 1.0 mM), the apparent charge transfer is derived as (4.0 ± 0.5) × 10^{-4} cm s^{-1} (Figure 2d). From the approach curves the thickness of diffusion layer (δ) is about 150 μm. If the diffusion coefficient of O_2 (Do_2) is adopted as 1.80 × 10^{-5} cm^2 s^{-1}, the mass transfer rate is derived as 1.2 × 10^{-3} cm s^{-1} (Do_2/δ). It can be concluded that, even if the solubility of O_2 is low in aqueous solution (0.25 mM), the photoelectrochemical conversion rate is limited by the interfacial charge transfer, i.e., the low kinetic rate of O_2 reduction at the TiO_2/solution interface. Thus, to promote the photoelectrochemical conversion rate, the simplest way is to use an electron acceptor with faster kinetic rate.

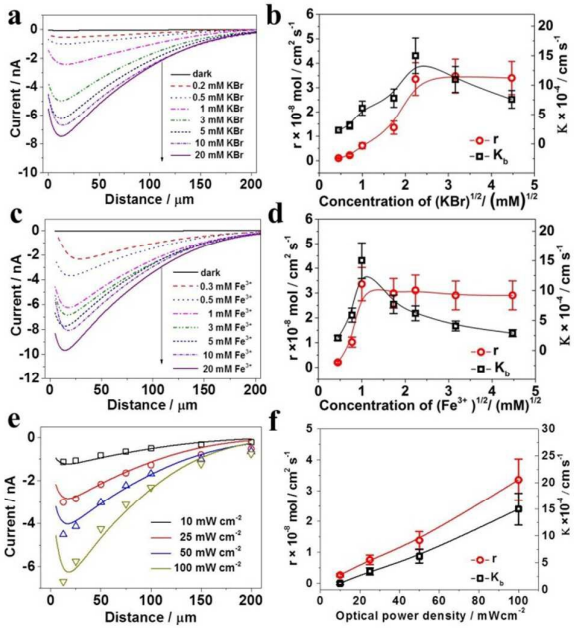

Figure 3 (a) Approach curves obtained in an aqueous solution with 50 mM H_2SO_4, 1 mM Fe^{3+} and different concentration of KBr. (b) Relationship between the concentration of KBr and the simulated apparent rate r (o) as well as apparent rate constant K_a (□). (c) Approach curves obtained in an aqueous solution with 50 mM H_2SO_4, 5 mM KBr and different concentration of Fe^{3+}. (d) Relationship between the con centration of Fe^{3+} and the simulated apparent rate r (o) as well as apparent rate constant K_a (□). (e) Approach curves obtained in 50 mM H_2SO_4, 5 mM KBr and 1 mM Fe^{3+} solution with different light intensity (spot: experimental, line: simulated). (f) Relationship between light intensity and the simulated apparent rate *r* (o) as well as apparent rate constant K_a (□) in 0.05 M H_2SO_4, 5 mM KBr and 1 mM Fe^{3+} solution. The tip potential is held at 0.7 V vs. Ag/AgCl reference electrode in experiment. The illumination intensity is 100 mW/cm^2 in (a) and (b).

So we adopt Fe^{3+} as electron acceptor. The photoelectrochemical reactions are formulated as followed:

$$Fe^{3+} + e^- \rightarrow Fe^{2+} \quad (4)$$

$$Br^- + h^+ \rightarrow 1/2 Br_2 \quad (2)$$

Distinct from TiO_2/(O_2, Br^-) system, a subsequently homogeneous reaction will occur to regenerate Fe^{3+} and Br^-:

$$1/2 Br_2 + Fe^{2+} \rightarrow Br^- + Fe^{3+} \quad (5)$$

Similarly, the apparent photoelectrochemcial conversion rate is deduced as followed (details see S2)[19, 20]:

$$r = K_a [Br^-]^{1/2} [Fe^{3+}]^{1/2} \quad (6)$$

Where, K_a is the apparent kinetic rate of interfacial charge transfer, [Br^-] and [Fe^{3+}] are the interfacial concentration of Br^- and Fe^{3+}.

As shown in Figure 3a, when the concentration of Fe^{3+} is fixed at 1 mM, the feedback current keep increasing with the increased concentration of Br^-. When the concentration of Br^- is 5.0 mM, the feedback current is more than one order of magnitude higher than the limit of TiO_2/(O_2, Br^-) system. On the other hand, Figure 3c shows that if the concentration of Br^- is fixed 5.0 mM, in presence of 0.3 mM Fe^{3+} the feedback current is higher than that in the O_2-saturated solution containing 20.0 mM Br^-. With 1.0 mM Fe^{3+}, the feedback current increases by one order of magnitude. The results show that TiO_2/(Fe^{3+}, Br^-) system has an excellent capability to produce Br_2. From the simulation results shown in Figure 3b and 3d,

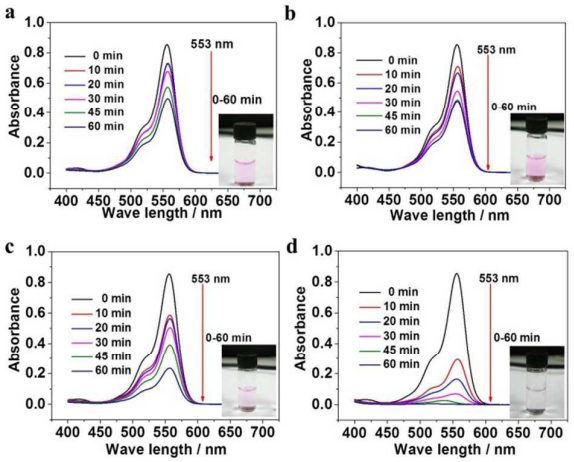

Figure 4 UV-visible spectrum of the TiO_2 photodegradation of Rhodamine B in different illumination time with different aqueous solution: (a) 50 mM H_2SO_4, 5.0 mM KBr and saturated O_2; (b) 50 mM H_2SO_4, 1.0 mM Fe^{3+}; (c) 50 mM H_2SO_4, 5.0 mM KBr and 0.25 mM Fe^{3+}; (d) 50 mM H_2SO_4, 5.0 mM KBr and 1.0 mM Fe^{3+}. The initial concentration of Rhodamine B is 10 mg/L, the illumination intensity is 100 mW cm^{-2}, and the diameter of illumination region of TiO_2 photoelectrode is 5 mm.

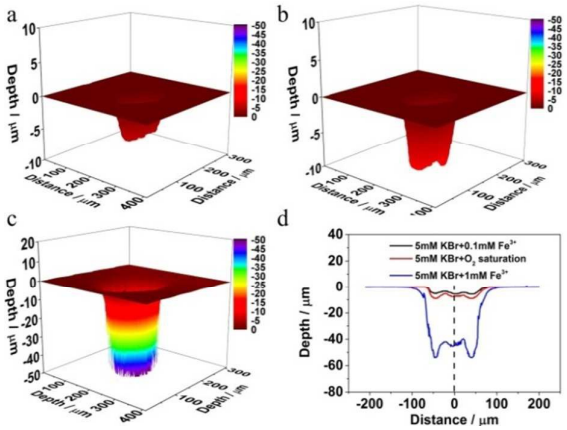

Figure 5 Confocal laser scanning microscopic images of the photochemical etching pits in different aqueous solutions: (a) 50 mM H_2SO_4, 5 mM KBr and 0.1 mM Fe^{3+}, (b) 50 mM H_2SO_4, 5mM KBr and saturated O_2, (c) 50 mM H_2SO_4, 5mM KBr and 1 mM Fe^{3+}. The initial distance between the Pt microelectrode and GaAs is 1 μm. The light intensity from Xenon light is 100 mW·cm^{-2}. Etching time: 60 min. (d) The cross-section profiles of the photochemical etching pits obtained through confocal laser scanning microscope.

it is observed that, when the concentration of one redox mediator is fixed, the apparent photochemical reaction rate (r) will increase firstly and then become constant with the increasing concentration of the other. However, the apparent rate constant (K_a) will increase firstly and then decrease, which might indicate a change of rate-determining step (rds).

From Figure 3b and 3d, TiO_2/(1.0 mM Fe^{3+}, 5.0 mM Br^-) is suggested as the optimized photoelectrochemical system with the apparent rate constant (K_b) of (1.5 ± 0.5) × 10^{-3} cm s^{-1}. The apparent homogeneous reaction rate between Fe^{2+} and Br_2, K_{homo}, is also obtained as (6.5 ± 0.5) × 10^2 dm^3 mol^{-1} s^{-1}. It is well known that Fe^{3+}/Fe^{2+} and Br_2/Br^- are pretty reversible redox couples in electrochemistry (K > 10^{-2} cm s^{-1}). Meanwhile, the interfacial mass transfer is dramatically enhanced due to the subsequently homogeneous reaction (5). The results show that the inversion of K_a is due to the incomplete turnover of tip-generated Br^- at the TiO_2/solution interface, where the rate is limited by the available charges on the surface of illuminated TiO_2 nanoparticles.[21] In other words, for TiO_2/(1.0 mM Fe^{3+}, 5.0 mM Br^-) system, the rds is the balance of the charge separation and recombination processes on the TiO_2 photocatalyst.

Net production of Br_2 can be obtained by illuminating the TiO_2/(1.0 mM Fe^{3+}, 5.0 mM Br^-) system. When a drop of N,N-dimethyl-p-phenylenediamine (DPD) is added in after 20-minute-illumination, the color of the electrolyte changes from light yellow to pink (See figure S5). Since Br_2 is an importantly strong oxidant, this system is tested in green chemistry. Figure 4a shows the photodegradation of Rhodamine B by Br_2 while saturated O_2 is employed as the electron acceptor, while Figure 4b shows the direct photodegradation of Rhodamine B by TiO_2 while Fe^{3+} is employed as the electron acceptor. Comparing them with each other, there is not much difference in photodegradation rates. However, once saturated O_2 is replaced by 0.25 mM Fe^{3+}, the photodegradation rate is accelerated dramatically in presence of 5.0 mM Br^- (Figure 4c). When the concentration of Fe^{3+} is increased to 1.0 mM, Rhodamine B is degraded completely in 60 minutes (Figure 4d).

Suppose it is a quasi-one order reaction, the photodegradation rate can be obtained through the linear relationship between $\ln(C_t/C_0)$ and the illumination time t.[22] The photodegradation rate of Rhodamine B by the synergetic effect of TiO_2/(1.0 mM Fe^{3+}, 5.0 mM Br^-) system is obtained as 0.139 min^{-1}, which is one order higher than that of TiO_2/(saturated O_2, 5.0 mM Br^-) system (0.013 min^{-1}) (More datails see Figure S9). When this competitive reaction is introduced, a new equilibrium should be established for the whole system, wherein the mass transfer of Br^- is enhanced by the homogenous reaction between Br_2 and Rhodamine B, which can be compensated sufficiently by the reduction of Fe^{3+}. Note that in these experiments the solution is not degassed. That means the produced Fe^{2+} can be easily oxidized to Fe^{3+} by dissolved O_2, the photogenerated Br_2 or even the holes on TiO_2 surface. The newly established equilibrium ensures both mass and charge balance in the degradation processes. A schematic diagram is shown in Figure S5b. The results elucidate that synergetic effect enhanced photoelectrocatalysis has potential applications in environment domains.

As a classic etchant used in semiconductor industry, the in-situ generation of Br_2 is valuable in the fabrication of three dimensional microstructures.[23, 24] Gallium arsenide (GaAs) is a direct bandgap semiconductor with a zinc blende crystal structure, which is used in the manufacture of devices such as integrated circuits, infrared light-emitting diodes, laser diodes, solar cells and optical windows.[25-28] The TiO_2/(Fe^{3+}, Br^-) system is employed for photoelectrochemical etching of GaAs wafer. A TiO_2 loaded optic fiber (diameter: 100 μm) is used as the etching tool to generate the etchant Br_2, which reacts with GaAs to fabricate microstuctures:

$$3Br_2 + GaAs + 3H_2O \rightarrow Ga^{3+} + AsO_3^{3-} + 6Br^- + 6H^+ \quad (7)$$

Although this reaction is competitive with Reaction (5), a new equilibrium will be set up as analyzed above (See also Figure S5b). Figure 5a-5c give three images of the etching pits obtained at different concentration of Fe^{3+} and Br^- while Figure 5d shows the profile of each etching pit. When the concentration of Fe^{3+} is lower than that of saturated O_2, the etching depth of TiO_2/(Fe^{3+}, Br^-) system (7.2 μm) is smaller than that of TiO_2/(saturated O_2, Br^-)

system (8.5 μm) within the etching time of 60 min. That means, in this case, the interfacial transfer of photogenerated electrons is the rds due to insufficient mass transfer of Fe^{3+} at the TiO_2/solution interface, which hinders the removal of holes by Br^- to generate Br_2 for GaAs etching. If the concentration of Fe^{3+} is increased to 1 mM, the etching depth of TiO_2/(Fe^{3+}, Br^-) system (40.5 μm) is almost five times higher than that of TiO_2/(saturated O_2, Br^-) system within the same etching time of 60 min. The etching rate in Z-axis is improved from 141 nm/min to 675 nm/min due to the synergetic effect of TiO_2/(Fe^{3+}, Br^-) system. This result may open the photochemical lithography on the microfabrications in semiconductors industry.

In summary, aside the interfacial structure of photoelectrode, we emphasize the importance of interfacial reaction system on the promotion of charge transfer efficiency of photoelectrochemcial system. If Fe^{3+} and Br^- are adopted as the acceptors of electrons and positive holes, they can be regenerated through the subsequently homogeneous reaction between Fe^{2+} and Br_2, the products of the interfacial transfer of photogenerated charges. The mass transfer loop increases the fluxes of Fe^{3+} and Br^- at the TiO_2/solution interface and, consequently, promotes the charge transfer capacity. The kinetic rate of interfacial charge transfer is enhanced dramatically. This phenomenon is termed as synergetic effect enhanced photoelectrocatalysis. The distinct advantage lies in that there is not net consumption of the precursors. From the results of the photogradation of Rhodamine B as well as the in-situ etching of GaAs wafer, it can be concluded that the synergetic effect can promote the efficiency of photoelectrochemical conversion, which has expectable utilizations of solar energy in green chemistry, microfabrication, and energy and environment domains.

The financial support by the National Basic Research Program of China (Grant 2012CB932902), the National Science Foundation of China (Grant 21327002, 91323303, 51205333, 91023047, 21273182 and 21321062), the Natural Science Foundation of Fujian Province of China (Grant 2012J06004), and the Program for New Century Excellent Talents in University (NCET-12-0318) are appreciated.

Notes and references

‡ J.C Jia and J. Zhang contributed equally to this work. All authors have given approval to the final version of the manuscript. The authors declare no competing financial interest.

1. N. Armaroli and V. Balzani, *Angew. Chem. Int. Ed.*, 2007, **46**, 52-66.
2. A. Fujishima and K. Honda, *Nature*, 1972, **238**, 37-38.
3. B. Oregan and M. Gratzel, *Nature*, 1991, **353**, 737-740.
4. M. Kapilashrami, Y. Zhang, Y.-S. Liu, A. Hagfeldt and J. Guo, *Chem. Rev.*, 2014, **114**, 9662-9707.
5. W. L. Ma, C. Y. Yang, X. Gong, K. Lee and A. J. Heeger, *Adv. Funct. Mater.*, 2005, **15**, 1617-1622.
6. R. J. Ellingson, M. C. Beard, J. C. Johnson, P. R. Yu, O. I. Micic, A. J. Nozik, A. Shabaev and A. L. Efros, *Nano Lett.*, 2005, **5**, 865-871.
7. C. J. Brabec, N. S. Sariciftci and J. C. Hummelen, *Adv. Funct. Mater.*, 2001, **11**, 15-26.
8. A. L. Linsebigler, G. Lu and J. T. Yates Jr, *Chem. Rev.*, 1995, **95**, 735-758.
9. J. Schneider, M. Matsuoka, M. Takeuchi, J. Zhang, Y. Horiuchi, M. Anpo and D. W. Bahnemann, *Chem. Rev.*, 2014, **114**, 9919-9986.
10. H. Zhou, Q. Chen, G. Li, S. Luo, T.-b. Song, H.-S. Duan, Z. Hong, J. You, Y. Liu and Y. Yang, *Science*, 2014, **345**, 542-546.
11. C. Wang and D. Astruc, *Chem. Soc. Rev.*, 2014, **43**, 7188-7216.
12. R. Dabestani, X. Wang, A. J. Bard, A. Campion, M. A. Fox, S. E. Webber and J. M. White, *J. Phys. Chem.*, 1986, **90**, 2729-2732.
13. A. M. El-Hamouz and R. Mann, *Ind. Eng. Chem. Res.*, 2007, **46**, 3008-3015.
14. K. Tanaka and F. Toda, *Chem. Rev.*, 2000, **100**, 1025-1074.
15. J. Patrin, Y. Li, M. Chander and J. Weaver, *Appl. Phys. Lett.*, 1993, **62**, 1277-1279.
16. C. Cha and J. Weaver, *J. Vac. Sci. Technol. B*, 1996, **14**, 3559-3562.
17. J. M. Kesselman, G. A. Shreve, M. R. Hoffmann and N. S. Lewis, *J. Phys. Chem.*, 1994, **98**, 13385-13395.
18. B. Reichman and C. E. Byvik, *J. Phys. Chem.*, 1981, **85**, 2255-2258.
19. S. M. Fonseca, *Development of scanning electrochemical microscopy for the investigation of photocatalysis at semiconductor surfaces*, University of Warwick, 2002.
20. S. M. Fonseca, A. L. Barker, S. Ahmed, T. J. Kemp and P. Unwin, *PCCP*, 2004, **6**, 5218-5224.
21. S. K. Haram and A. J. Bard, *J. Phys.Chem. B*, 2001, **105**, 8192-8195.
22. X. Yu, A. Shavel, X. An, Z. Luo, M. Ibáñez and A. Cabot, *J. Am. Chem. Soc.*, 2014, **136**, 9236-9239.
23. Y. Tarui, Y. Komiya and Y. Harada, *J. Electrochem. Soc.*, 1971, **118**, 118-122.
24. M. Beerbom, T. Mayer and W. Jaegermann, *J. Phys. Chem. B*, 2000, **104**, 8503-8506.
25. M. S. Shur, *GaAs devices and circuits*, Springer Science & Business Media, 2013.
26. J. Yoon, S. Jo, I. S. Chun, I. Jung, H.-S. Kim, M. Meitl, E. Menard, X. Li, J. J. Coleman and U. Paik, *Nature*, 2010, **465**, 329-333.
27. L. Zhang, X. Z. Ma, J. L. Zhuang, C. K. Qiu, C. L. Du, J. Tang and Z. W. Tian, *Adv. Mater.*, 2007, **19**, 3912-3918.
28. O. Ueda, *Microelectron. Reliab.*, 1999, **39**, 1839-1855.